Exact statistical model accounting for surface fluctuations in two-dimensional droplets

E. van Faassen
Department of Molecular Biophysics, Buys Ballot Laboratory,
Utrecht State University, P.O. Box 80.000, 3508 TA, Utrecht, The Netherlands
(Received 14 September 1992)

In a soluble model we investigate the role of geometrical shape fluctuations for the equilibrium properties of a polydisperse ensemble of two-dimensional droplets. Interactions within a droplet include bending rigidity and spontaneous curvature. Interactions between droplets are omitted. Taking rigorous account of all possible shapes of the individual droplets, the droplet-size distribution is found for arbitrary temperature. The fluctuation-dominated regime extends to temperatures far lower than expected from a mean-field calculation.

PACS number(s): 68.35.Rh, 05.20.−y, 82.70.−y

Recent years have seen intensive research efforts devoted to the study of the equilibrium properties of amphiphilic systems, emulsions, or other realizations of interfaces between two phases. These systems have been shown to exhibit a rich phase behavior [1]. Great interest is concentrated on the role of geometrical fluctuations of the interface around the most probable configuration, i.e., the configuration which minimizes the Hamiltonian. This is motivated by the fact that, for interfaces and embedding spaces of low dimension, fluctuations should be far from negligible. For amphilic systems this question is particularly acute since many realistic systems exhibit small surface bending rigidities of the order of thermal excitations. In that case the thermodynamic properties should be strongly affected by fluctuations of the shape of the surface.

From the theoretical side, the role of shape variation has been mostly studied in planar configurations of unbounded sheets. One of the most interesting conclusions was the realization [2,3] that the microscopic parameters entering the Hamiltonian (e.g., bending rigidity) are strongly renormalized when considered on a certain length scale, this renormalization being caused by surface fluctuations taking place on smaller scales. Many other interesting entropic phenomena have since been identified.

On the other hand, experimental studies [4,5] are obviously restricted to finite, though possibly large, surfaces. In many cases, extra conditions like spherical shape or given total surface area will act as strong geometrical constraints on the interface: A typical suspension will comprise a large number of aggregates of spherical topology, and these aggregates come with a wide variety of shapes and sizes [6].

Such finite aggregates have been considered in detailed but time consuming simulations of the fluctuation dynamics of a single isolated vesicle in both two [7] and three [8] dimensions, but extension of these results to the polydisperse case seems impractical at the moment. The implications of small distortions of spherical vesicles in a polydisperse emulsion have been considered [9] analytically some time ago. Progress on the problem of incorporating large shape distortions has been lacking, however. The obvious reason lies in the difficulty of accounting for the constraint of spherical topology, as this constraint introduces effective long-range interactions between all molecules in the vesicle.

We therefore formulate a highly idealized model for a suspension, which rigorously accounts for closedness, polydispersity in aggregate size, as well as for arbitrary shapes a particular aggregate might find itself in. In what follows we will refer to an aggregate as a droplet, irrespective of its shape or topology.

The problem of calculating the total partition function separates into two parts: First, for any particular droplet size, the summation over all geometrical configurations has to be carried out in compliance with the geometrical constraints. Second, the resulting free energy for a particular droplet size subsequently enters as the weight of a suitable defined grand canonical sum over all droplet numbers and sizes.

For reasons to be given below, we consider droplets containing five or more particles only. Let us denote with n_N the number of droplets of size N, and neglect the interactions between individual droplets. The calculation is most conveniently carried out in the grand canonical average defined as the sum over all sets of nonnegative numbers n_N compatible with a given total number of droplets $M_0 \equiv \sum_N n_N$. Neglecting interactions between the various droplets, this average is given by

$$
\begin{aligned}
e^{-\beta\Omega} &= \sum_{\{n_N\}=0}^{\infty *} \frac{1}{n_5! n_6! \cdots n_N! \cdots} \prod_{N=5}^{\infty} e^{-\beta(F_N-\mu N)n_N} \\
&= \frac{1}{M_0!}\left[\sum_{N=5}^{\infty} e^{-\beta(F_N-\mu N)}\right]^{M_0} \\
&= \frac{1}{M_0!} D(\beta,\mu)^{M_0} \, . \qquad (1)
\end{aligned}
$$

Here the last line serves as the definition of the function D, μ denotes the chemical potential for a single particle, and F_N stands for the free energy of a droplet containing N particles. The counting factor accounts for the mixing

entropies of the various droplet types [10]. The form of Eq. (1) guarantees that all averages over the chosen ensemble will be proportional to the total number of droplets M_0. Therefore, D is seen to be the proper normalization factor for the probabilities P_N to find a droplet consisting of N particles,

$$P_N(\beta,\mu)=D^{-1}e^{-\beta(F_N-\mu N)} . \tag{2}$$

This droplet-size distribution still depends on the chemical potential μ, which may be adjusted to obtain a desired average number of particles per droplet, $\bar{N}$,

$$\bar{N}\equiv\sum_{N=5}^{\infty} NP_N . \tag{3}$$

In order to specify F_N, we treat an N-particle droplet as a closed chain of sticks, connected at the end points. In what follows, we assume the chain to be restricted to the plane, although the generalization to an embedding space of higher dimension is straightforward [11]. The corresponding N-chain Hamiltonian consists of the bending energy, characterized by a bending rigidity κ and spontaneous curvature a, as both concepts are crucial for the characteristic properties of emulsion interfaces [1]. We choose a widely used form that is equivalent to the classical planar Heisenberg chain in the absence of external fields,

$$H_N(\Delta_1,\ldots,\Delta_N)=\kappa\sum_{i=1}^{N}1-\cos(\Delta_i-a) , \tag{4}$$

where $\Delta_i\in[-\pi,\pi]$ is the angular increment of the interface at the ith vertex. From this N-chain Hamiltonian we define a (complex) partition function $Z_N(\alpha)$ as a sum over all configurations consistent with the requirement that the chain be closed. However, we will not exclude the possibility that the droplet intersects itself (ghost interface).

$$Z_N(\alpha)=\int_{-\pi}^{\pi}\prod_{i=1}^{N}\frac{d\Delta_i}{2\pi}e^{-\beta H_n}\delta\left[\sum_{i=1}^{N}\cos\sigma_i\right]\times\delta\left[\sum_{i=1}^{N}\sin\sigma_i\right]e^{-i\alpha(\sigma_N-\sigma_1)} , \tag{5a}$$

$$\sigma_i\equiv\sum_{n=1}^{i}\Delta_n \tag{5b}$$

This partition function contains the contributions from all configurations with arbitrary integer values for the winding number $W\equiv(\sigma_N-\sigma_1)/2\pi$ ($W\in\mathbb{Z}$). This motivates the introduction of the last exponential in the integrand: It gives a characteristic phase factor $e^{-i\alpha 2\pi W}$ to each topological subclass of winding number W. Therefore, the contribution from a particular winding number W_0 may be projected out by an integral over the topological angle α,

$$e^{-\beta F_N}|_{W_0}=\int_0^1 d\alpha\, e^{i\alpha 2\pi W_0}Z_n(\alpha) . \tag{6}$$

These free energies may then be used in Eq. (2) to compute the size distribution of droplets with the selected winding number, or any other desired thermodynamic average. At first sight the appearance of a complex integrand in Eq. (6) seems unphysical until one realizes that the periodicity in the topological angle α implies the relation $Z_N(1-\alpha)=Z_N(\alpha)^*$. This guarantees positive real values for the total integral and meaningful results for the free energies F_N.

As it stands, the $(N-2)$-fold integration in Eq. (5a) is difficult to evaluate due to the δ-function constraints that introduce a strong coupling between all particles in the droplet. However, using a Laplace transform method analogous to the solution of the Berlin-Kac model for ferromagnetic spin systems [12], the constraints may be brought into a factorized form,

$$\begin{aligned}\delta\left[\sum_{i=1}^{N}\cos\sigma_i\right]\delta\left[\sum_{i=1}^{N}\sin\sigma_i\right]&=\int_{-\infty}^{\infty}\frac{ds}{2\pi}\frac{dt}{2\pi}\exp\left[is\left[\sum_{i=1}^{N}\cos\sigma_i\right]\right]\exp\left[it\left[\sum_{i=1}^{N}\sin\sigma_i\right]\right]\\&=\frac{1}{2\pi}\int_0^{\infty}\rho\,d\rho\int_0^{2\pi}\frac{d\varphi}{2\pi}\exp\left[i\rho\sum_{i=1}^{N}\cos(\varphi-\sigma_i)\right] ,\end{aligned} \tag{7}$$

where ρ and φ are the polar coordinates in the two-dimensional (2D) integration space. Using transfer-matrix techniques [13], a lengthy algebraic manipulation transforms the partition function into the polar integral over a trace. As this trace is independent of the polar angle φ, the latter integration may be done at once, and the result may be compactly written as

$$Z_N(\alpha)=\frac{1}{2\pi}\int_0^{\infty}\rho\,d\rho\,\mathrm{tr}T^N(\alpha,\rho) , \tag{8a}$$

where the transfer operator $T(\alpha,\rho)$ is defined as

$$T\psi(y)=\int_{y-\pi}^{y+\pi}\frac{dz}{2\pi}e^{-\beta\kappa[1-\cos(z-y-a)]}e^{i\rho\cos(z)}e^{-i\alpha z}\psi(z) . \tag{8b}$$

The three exponentials in the integrand have the following significance: The first accounts for the vertex interaction as given by the Hamiltonian Eq. (4). The second accounts for the geometrical constraint that the aggregates be closed. The third exponential provides the topological decomposition into subclasses with definite winding number.

For numerical studies of Eqs. (8a) it is convenient to expand the transfer operator on the basis of harmonic functions within period 2π. Omitting a nonessential phase factor which does not affect the final trace in Eq. (8a), the matrix elements may be expressed in terms of Bessel functions $J_m(\rho)$ and the Fourier coefficients $E_l(\alpha)$ of the vertex interaction,

$$T_{lm}(\alpha,\rho)=E_l(\alpha)J_{m-l}(\rho) , \tag{9a}$$

$$E_l(\alpha)=\int_{-\pi}^{\pi}\frac{dz}{2\pi}e^{-\beta\kappa[1-\cos(z-a)]}e^{-i(l+\alpha)z} . \tag{9b}$$

From these expressions the traces over the transfer matrices were computed recursively by brute force matrix multiplication. Subsequent integration over the geome-

trical parameter ρ and the topological angle α were implemented with a standard Gaussian integration procedure. The asymptotic behavior of the Bessel functions guarantees convergence of the geometrical integral for droplet sizes exceeding five particles. This property motivates the choice of five as the minimal droplet size included in the grand canonical summation [cf. Eq. (1)].

Figure 1 shows predictions for the size distribution P_N of the droplets. For all calculations presented in this Brief Report, the spontaneous curvature was chosen $a=0.5$, and the winding number set to $W_0=1$. The distribution has been normalized to unity and its first moment $\bar{N}$ has been set to 15 by adjusting the chemical potential μ. The importance of geometrical fluctuations may be seen by comparing these exact results with a mean-field approximation (MFA). It is formulated in terms of the energy of the regular N-sided polygon with bending angle $\vartheta_N=2\pi W_0/N$ at all vertices. The corresponding Boltzmann factor is multiplied with the available phase-space volume V_N,

$$e^{-\beta F_N}\equiv V_N e^{-\beta\kappa N[1-\cos(\vartheta_N-a)]}, \quad \text{MFA}, \tag{10}$$

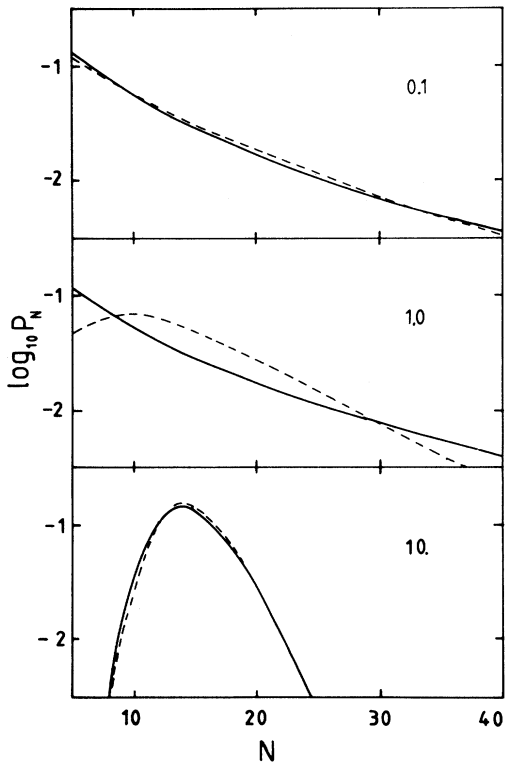

FIG. 1. Logarithm of the normalized droplet-size probabilities P_N at three temperatures ($\beta\kappa=0.1$, 1.0, and 10.0, respectively). The curvature was chosen $a=0.5$, and the chemical potential adjusted to give an average droplet size of $\bar{N}=15$. Solid curves are predictions from the exact calculation, dashed curves result from the MFA.

$$V_N\equiv\int_0^1 d\alpha e^{i\alpha 2\pi W_0}\int_{-\pi}^{\pi}\prod_{i=1}^{N}\frac{d\Delta_i}{2\pi}\delta\left[\sum_{i=1}^{N}\cos\sigma_i\right]\times\delta\left[\sum_{i=1}^{N}\sin\sigma_i\right]e^{-i\alpha(\sigma_N-\sigma_1)}. \tag{11}$$

This mean-field description ensures good agreement with the exact calculation at very high temperatures, provided the Hamiltonian is bounded, as in Eq. (4). At such temperatures the system behaves purely entropically, i.e., dominated by the available phase-space volume. At intermediate temperatures the Boltzmann factor gains importance and serious discrepancies between the exact and the MFA calculations arise. At very low temperatures, the exact result is dominated by small geometrical fluctuations around the regular polygon. As this polygon appears explicitly in the mean-field prescription, the MFA is accurate in this temperature regime also.

As expected, the effects from shape fluctuations manifest themselves most prominently in the crossover regime $\beta\kappa\cong 1$, where the thermal excitations are of the order of the bending energies in the droplets. From high temperatures right into the crossover regime, the shape fluctuations in the exact model are so dominant as to completely overshadow the Hamiltonian contribution to the free energy. This may be seen from the close similarity of the droplet-size distributions at $\beta\kappa=0.1$ and 1. This point is illustrated even more clearly by the spread ΔN in aggregate size as a function of temperature,

$$(\Delta N)^2\equiv\overline{(N-\bar{N})^2}. \tag{12}$$

The results are given in Fig. 2. The MFA is seen to retain temperature dependence throughout the temperature range considered. The exact calculation shows a marked absence of any temperature effect for $\beta\kappa<1$, indicating that the size distribution is not affected by the details of the Hamiltonian, but is fully determined by the available phase space only. In itself, it is not surprising that these

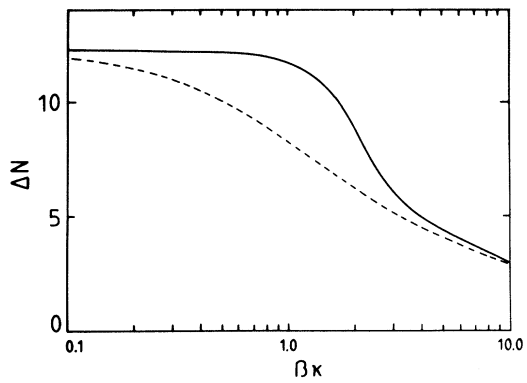

FIG. 2. Spread ΔN in droplet-size distribution as defined by Eq. (12). Curves are labeled as in Fig. 1. In mean-field approximation the spread retains temperature dependence, whereas the exact calculation shows the spread to be insensitive to temperature (and therefore the Hamiltonian) as soon as $\beta\kappa<1$.

entropic contributions dominate in the high-temperature regime. It is remarkable, however, that this dominance extends down to temperatures where $\beta\kappa \cong 1$.

The exactly soluble model described above may be generalized in a number of ways: For example, it may be formulated for embedding spaces of dimension exceeding 2, as well as with more general vertex interactions. For such a general vertex potential $\kappa V(\Delta_i - a)$, the Fourier coefficients E_l should read

$$E_l(\alpha) = \int_{-\pi}^{\pi} \frac{dz}{2\pi} e^{-\beta\kappa V(z-a)} e^{-i(l+\alpha)z} . \tag{13}$$

An interesting application of this generalization arises with a vertex potential forcing the curvature to have definite signature, say positive. In combination with the closedness of the aggregates and unit winding number, this choice yields a self-avoiding statistical model, results for which will be presented elsewhere.

The lack of self-avoidance [14] in the model as implied by Eq. (5a) clearly points out severely unrealistic aspects of the current calculation. A further undesirable feature is the obvious fact that the 1D structures considered here are rather poor analogs of realistic droplets or vesicles. Obviously lacking also are contributions from pressure differentials between the two sides of the micelle surface that are expected to play an important role in droplet stabilization [7]. Finally, the size distribution function should in principle be affected by the presence of even very weak interactions between individual droplets as they arise from electromagnetic [15] or geometrical [16,17] fluctuations. However, whereas such interactions will strongly affect the overall thermodynamic behavior of the ensemble, the actual effect on the droplet-size distribution might not be severe. For example, inclusion of the interdroplet interactions via a mean-field formalism will result in an interaction depending on the total amount of amphiphile, but not on the way this amount is distributed over the various droplet sizes. This leaves the droplet-size distribution unchanged unless the interactions between the droplets are sufficiently strong to induce, say, a phase separation into a dilute and a concentrated phase.

None of the physical ingredients mentioned above have been included in the current calculation. In spite of these severe shortcomings, the attraction of the model presented above lies in the rigorous incorporation of shape fluctuations of the interface, while retaining the strong geometrical and topological constraints of closedness and specified winding number. After all, these constraints involve all particles in a given aggregate simultaneously, and thereby introduce effective long-range interactions between them. Finally, being exactly soluble, the current model will be used to investigate the consequences of a number of approximate treatments as found in the literature.

[1] For a recent review, see *Statistical Mechanics of Membranes and Surfaces,* edited by D. Nelson, T. Piran, and S. Weinberg (World Scientific, Singapore, 1989).

[2] P. G. de Gennes and C. Taupin, J. Phys. Chem. **86**, 2294 (1982).

[3] L. Peliti and S. Leibler, Phys. Rev. Lett. **54**, 1690 (1985).

[4] *Physics of Amphiphilic Layers,* edited by J. Meunier, D. Langevin, and N. Boccara (Springer, Berlin, 1987).

[5] *The Structure and Conformation of Amphiphilic Membranes,* edited by R. Lipowski, D. Richter, and K. Kremer (Springer, Berlin, 1992).

[6] *Surfactants in Solution,* edited by K. Mittal and B. Lindman (Plenum, London, 1987).

[7] S. Leibler, R. Singh, and M. Fisher, Phys. Rev. Lett. **59**, 1989 (1987).

[8] A. Baumgartner and J. Ho, Phys. Rev. A **41**, 5747 (1990).

[9] S. A. Safran, J. Chem. Phys. **78**, 2073 (1983).

[10] See A. Sommerfeld, *Thermodynamik und Statistik* (Verlag H. Deutsch, Thun, 1977), Chap. 29.

[11] The case of large unconstrained chains is treated by M. Fisher, Am. J. Phys. **32**, 343 (1964).

[12] T. Berlin and M. Kac, Phys. Rev. **86**, 821 (1952).

[13] See J. Kogut, Rev. Mod. Phys. **51**, 659 (1979).

[14] M. Kardar and D. Nelson, Phys. Rev. A **38**, 966 (1988); B. Duplantier, in *Statistical Mechanics of Membranes and Surfaces* (Ref. [1]), p. 226.

[15] J. Israelachvili, *Intermolecular and Surface Forces* (Academic, Orlando, 1985).

[16] W. Helfrich, Z. Naturforsch. A **33**, 305 (1978).

[17] F. David, J. Phys. IV (Paris) Colloq. **67**, 115 (1990).